RSC Advances

ROYAL SOCIETY OF CHEMISTRY

www.rsc.org/advances

A study on deactivation of Cu-Zn-Al catalyst for higher alcohols synthesis

Yongjun Liu, Chaobo Liu, Xuan Deng, Wei Huang*

Key Laboratory of Coal Science and Technology of Ministry of Education and Shanxi Province, Taiyuan University of Technology, Taiyuan 030024, Shanxi, China

Corresponding author. Tel. /fax: +86 351 6018073

E-mail address: huangwei@tyut.edu.cn (W. Huang)

Abstract

Cu-Zn-Al catalyst without promoters, was prepared by complete liquid-phase method and tested for a deactivation study in higher alcohols synthesis from syngas. Results showed that the selectivity of higher alcohols first increased from 36.0 % to 68.6 % then gradually decreased to 14.1 % with time on stream. Characterization results showed that Cu species and Zn species had little changes whereas the phase of Al species changed after reaction. It was found that the Al species of Cu-Zn-Al catalyst changed from AlOOH to Al_2O_3. The phase change weakened CO dissociation and chain growth which led to the decrease of higher alcohols selectivity with time on stream. It was suggested that AlOOH had the function of CO dissociation and chain growth, which favored the formation of higher alcohols, whereas Al_2O_3 had no function of CO dissociation, which caused the formation of methanol.

Key words: CO hydrogenation; Higher alcohols; Cu-Zn-Al catalyst; Deactivation;

1. Introduction

Higher alcohols have received considerable interest recently because of its potential as fuel and substitute for gasoline [1,2]. Currently, Cu-based catalysts for higher alcohols synthesis (HAS) from syngas are Cu-Co or Cu-Fe bimetallic catalysts and alkalis modified methanol synthesis catalysts [3-5]. On Cu-Co or Cu-Fe bimetallic catalysts, the Cu-X (X=F-T elements) center is thought to be the active site (dual site) for higher alcohol synthesis [6,7]. And alkalis is considered to play a key role in the synthesis of higher alcohols over alkalis modified methanol synthesis catalysts [5].

It is well known that Cu-Zn-Al catalysts are usually used to synthesize methanol from CO or CO_2 hydrogenation [8,9]. Nonetheless, in our previous study, it was found that the selectivity of ethanol over Cu-Zn-Al catalysts without promoters could reach an unexpected point, however, the result is very difficult to reproduce [10]. At beginning, this novel phenomenon of ethanol formation over Cu-Zn-Al catalysts without promoters is ascribed to the synergism of Cu^0 and Cu^+ through experimental and theoretical studies [11,12]. But presently we have found that Al species is also playing a key role in the formation of higher alcohols, not just as the role of a carrier in the synthesis of methanol.

Therefore, in this paper, the Cu-Zn-Al catalyst without promoters was prepared by complete liquid-phase method and tested for a deactivation study in higher alcohols synthesis from syngas. To clarify the reason of catalyst deactivation, the structure of each metallic component of the catalyst was investigated before and after reaction. The correlation between the change of catalytic performance and the structural change was also discussed.

2. Experimental

2.1 Catalyst preparation

The Cu-Zn-Al slurry catalyst with the composition of Cu/Zn/Al= 2/1/0.8 (atomic ratio) was prepared by complete liquid-phase method. Typically, Aluminum isopropylate [$(C_3H_7O)_3Al$] was dissolved in a mixture of deionized water with a certain amount of citric acid at 323 K and maintained for 3 h, then the temperature was raised to 368 K and kept for 1 h. Next, the $Cu(NO_3)_2 \cdot 3H_2O$ and $Zn(NO_3)_2 \cdot 6H_2O$ were dissolved in glycol and the mixture was slowly added to the Al solution. The resulting Cu-Zn-Al solution was stirred at 368 K until a homogeneous sol was obtained. The sol was aged at room temperature for 10 days to obtain a gel. At last, the gel was dispersed in liquid paraffin, heated under N_2 atmosphere from 333 K to 573 K with a heating rate of 5 K/min and kept for 8 h at 573 K. Then a slurry catalyst was subsequently obtained.

2.2 Catalyst characterization

The slurry catalyst was centrifuged, extracted by petroleum ether and dried at room temperature before characterization.

Powder X-ray diffraction (XRD) patterns were recorded on a Rigaku D/MAX-2500 Diffractometer in a 2θ range of 5-85°. Fourier transform infrared spectra (FTIR) were obtained on an AVATAR 370 spectrometer. NH_3 temperature-programmed desorption (NH_3-TPD-MS) were performed to measure the basicity of the catalyst. ^{27}Al-MAS-NMR measurements were performed on a Bruker Avance DSX 500 spectrometer with a ^{27}Al frequency of 130.4 MHz. Graphite furnace atomic absorption spectrometry (GF AAS) were performed to quantify the composition of catalyst formulation by SpectrAA-220 AAS equipment. X-ray photoelectron spectroscopy (XPS) measurements were conducted using an ESCALAB 250 spectrometer. Thermogravimetric mass spectrometry (TG-MS) analyses were performed by a Setaram SETSYS TGA coupled with a

hiden HPR20 QIC R&D mass spectrometry.

2.3 Catalytic activity test

CO hydrogenation to higher alcohols was carried out in a slurry reactor with a mechanical magnetic agitator. The syngas (H_2/CO=2) was introduced into the reactor with a feed flow rate of 150 mL/min under 523 K, 4.5 MPa. The steady-state activity measurement was taken after at least 24 h on the stream. The gaseous products were analyzed online with a gas chromatograph equipped with a flame ionization detector (FID) to detect gaseous hydrocarbons and a thermal conductivity detector (TCD) to detect gaseous inorganic, respectively. The liquid products were collected daily and analyzed offline using the gas chromatograph.

3. Results and discussion

3.1. Catalytic performance

The catalytic performance of Cu-Zn-Al catalyst for CO hydrogenation at 523 K with time on stream (TOS) was listed in Table 1 and 2. CO conversion initially increased from 19.8 % at 24 h to 38.9 % at 48 h, then it gradually decreased to 32.0 % at 120 h with TOS. Meanwhile, the selectivity of total alcohols first decreased from 31.4 % to 14.0 % at 72 h and then increased to 22.1 % at 120 h. Notably, the selectivity of dimethyl ether (DME) increased gradually with TOS, and the selectivity of higher alcohols (C_{2+}OH/ROH) increased from 36.0 % at 24 h to 68.6 % at 48 h and then gradually decreased to 14.1 % at 120 h. Moreover, the selectivity of CH_3OH and CH_4 first decreased and then increased overall, which illustrated that the functions of catalyst for CO dissociation and propagation were weaken with TOS. The catalytic performance indicated that a deactivation happened on Cu-Zn-Al catalyst in higher alcohols synthesis and the reason for the catalyst deactivation would be clarified combining with the following characterization results.

3.2. XRD analysis

As discussed above, a deactivation happened on Cu-Zn-Al catalyst in the formation of higher alcohols from the catalytic performance. It was speculated that some structural changes occurred during the reaction. In order to confirm this speculation, the catalyst was subjected to analyse by XRD, FT-IR, NH_3-TPD-MS, ^{27}Al-MAS-NMR, XPS and TG-MS. Fig. 1 presented the XRD patterns of Cu-Zn-Al catalyst before and after reaction (meant after 120 h reaction in the whole manuscript). Only diffraction peaks of Cu^0 and ZnO could be detected, revealing that no new species were formed during 120 h reaction. The XRD results illustrated that the structure of Cu species or Zn species had little changes, which suggested that the deactivation of catalyst was not caused by the structural changes of Cu species and Zn species.

3.3. FT-IR analysis

Since the low content of Al in the catalyst, the diffraction peaks of Al species could not be detected by XRD. So the phases of Al species of Cu-Zn-Al catalyst before and after reaction were confirmed by FT-IR. As indicated in Fig. 2a, all absorption bands at 3414, 1629, 1423, 1327, 1089, 939, 769, 586 cm^{-1} were in agreement with the reported values of AlOOH, which confirmed the formation of AlOOH [13,14]. The intensive bands at 3414, 1089 and 1327 cm^{-1} belonged to the υ_{as} (Al)O-H, υ_s Al-O-H and υ_{as} Al-O-H vibrations of AlOOH, respectively. The three strong bands at 939, 769, and 586 cm^{-1} were ascribed to the vibration mode of AlO_6. The peak at 1423 cm^{-1} corresponded to OH stretching vibrations. The shoulder at 1629 cm^{-1} was the feature of the bending mode of absorbed water. In Fig. 2b, the intensive bands at 688 and 540 cm^{-1} were ascribed to Al-O stretching vibrations, which was the principal feature of Al_2O_3 [14,15]. The intensive band centered at 3434 cm^{-1} and weak band at 1598 cm^{-1} were attributed to

the stretching vibrations of OH groups in the hydroxide structure as well as the physically adsorbed water, respectively. All these facts confirmed that the phase of Al_2O_3 was obtained after reaction. The FT-IR analysis illustrated that the structure of Al species had changed from AlOOH to Al_2O_3 after 120 h reaction.

3.4. NH_3-TPD-MS analysis

Fig. 3 showed the NH_3-TPD-MS profiles of Cu-Zn-Al catalyst. As seen in Fig. 3, the amount of weak acid decreased after 120 h reaction. Busca et al [16] reported that the dehydration of hydroxyl groups would induce some freed and defective Al^{3+} ions and then increase the density of surface acid sites. This result indicated that the structure of Al species changed from AlOOH→ Al_2O_3, which accompanied by the dehydration reaction: $2AlOOH \rightarrow Al_2O_3 + H_2O$.

3.5. ^{27}Al-MAS-NMR analysis

Further evidence for the structural change of Al species before and after reaction could be obtained from the ^{27}Al-MAS-NMR spectra. Fig. 4 showed the ^{27}Al-MAS-NMR spectra of Cu-Zn-Al catalyst before and after reaction. As seen in Fig. 4, the resonance at approximately +8 ppm corresponded to the octahedral AlO_6 site of AlOOH [17,18]. And the resonance at +65 ppm was ascribed to the tetrahedral AlO_4 groups of Al_2O_3 [18]. This transformation in ^{27}Al NMR site illustrated that a proportion of Al in the octahedral sites (AlOOH) had transformed to tetrahedral sites (Al_2O_3).

3.6. AAS analysis

In order to confirm that the deactivation of catalyst was not caused by the change of catalyst composition, the composition of Cu-Zn-Al catalyst was analyzed by GF AAS and the results were listed in table 3. As we described in the catalyst preparation, the atomic ratio of Cu:Zn:Al was kept

at 2:1:0.8 theoretically. However, from the GF AAS results, it was calculated that the atomic ratio of Cu:Zn:Al was 1.8:1:0.3 before reaction and after reaction the atomic ratio of Cu:Zn:Al was 1.7:1:0.3. It could be seen that the composition of the catalyst before and after reaction was almost unchanged, which indicated that the catalyst deactivation was not caused by the change of catalyst composition. Since the slurry catalyst was centrifuged, extracted by petroleum ether, no matter before reaction or after reaction, the aluminum concentration was lower than theoretical composition, which might be the main reason why we could not detect either AlOOH or Al_2O_3 using XRD.

3.7. XPS analysis

In order to further confirm that the deactivation of catalyst was ascribed to the structural change of Al species rather than the Cu species and Zn species, the Cu-Zn-Al catalyst before and after reaction were analyzed by XPS and the binding energy (BE) of each component of the Cu-Zn-Al catalyst before and after reaction were present in Table 4. As shown in Table 4, the Cu2$p_{3/2}$ BE values were about 932.0 eV and no shake-up satellite peak between 940.0~945.0 eV (Fig. 5), which indicated the absence of Cu^{2+}, and the Zn2$p_{3/2}$ BE values were less than 1022.0 eV which could be assigned to ZnO [19, 20].This was consistent with the XRD results. However, the Al2*p* BE value before reaction was at 74.4 eV corresponding to Al-OH bonds, which was in agreement with Al in AlOOH [21]. After reaction, the BE of Al2*p* shifted to 73.7 eV corresponding to Al-O bonds which was considered as Al_2O_3 [21].

3.8. TG-DTG analysis

Fig.6 presented the TG-DTG profiles of the Cu/Zn/Al catalyst before and after reaction. As shown in Fig.6a, the thermal analysis of the Cu-Zn-Al catalyst showed four decomposition steps

before reaction. The first step at around 353 K was ascribed to desorption of physically adsorbed water. The weak DTG step at about 563 K was responsible for the loss of layer structural water of AlOOH. The strong step at about 713 K was attributed to the decomposition of AlOOH to γ-Al_2O_3 [22]. And the last step at about 1073 K was considered to be further conversion of γ-Al_2O_3 to other Al_2O_3. But after reaction, it could be found that the rate of weight loss decreased from DTG (curve b), especially for the step of AlOOH to γ-Al_2O_3, which illustrated that a proportion of AlOOH had converted to Al_2O_3 during reactions. Considering the reaction temperature was only 523 K, so further studies were required to figure out what caused such structural change, which might be beneficial to improve the stability of catalyst in the higher alcohols synthesis for our future work.

In order to direct prove that the formation of Al_2O_3 could deactivate the catalyst for the higher alcohol synthesis. A Cu-ZnO-Al_2O_3 catalyst was prepared using Al_2O_3 as Al source and compared it with the present study to investigate the formation of higher alcohols. The results were listed in table 5 and 6. As seen in table 5 and 6, the selectivity of higher alcohols was only 7.2 %, which was lower than that of the Cu-ZnO-AlOOH catalyst. This work further indicated that Al_2O_3 was not beneficial to the formation of higher alcohols. In addition, F. Schüth [23] et al prepared ternary Cu-ZnO-Al_2O_3 catalysts to obtain the greatest methanol synthesis activity. Wang [3] et al also prepared a serious of alumina-supported copper-cobalt catalysts to investigate the formation of higher alcohols, the results showed that methanol was the major product over monometallic Cu/γAl_2O_3.

It was widely accepted that a bi-functional (dual site) catalyst was required for higher alcohols formation, on which one acted as CO non-dissociative adsorption and insertion, while the other acted as CO dissociation and chain growth, the synergism between the dual site would benefit the

synthesis of higher alcohols [4,24,25]. In the stability study of this paper, the results showed that the CO conversion and the selectivity of higher alcohols first increased at early stage and then gradually decreased with time on stream, which was considered to be the structural change of catalyst according to the characterization results. It could be speculated that AlOOH had the function of CO dissociation and chain growth, which favored the formation of higher alcohols, whereas Al_2O_3 had no function of CO dissociation. As a result, the main reason for the decrease of higher alcohols selectivity was ascribed to the structural change of AlOOH→Al_2O_3.

4. Conclusion

The deactivation process and the structural change of Cu-Zn-Al catalyst before and after reaction were investigated. CO conversion and the selectivity of higher alcohols first increased at early stage and then gradually decreased with time on stream in HAS. During the reaction, a proportion of Al species of Cu-Zn-Al catalyst changed from AlOOH to Al_2O_3. Such structural change was the main reason for the deactivation of Cu-Zn-Al catalyst in the formation of higher alcohols. This result suggested that AlOOH had the function of CO dissociation and chain growth, which favored the formation of higher alcohols, whereas Al_2O_3 had no function of CO dissociation over Cu-Zn-Al catalyst without promoters.

Acknowledgements

This research was supported by Natural Science Foundation of China (21176167); the Key Project of Natural Science Foundation of China (21336006); and the Doctoral Program of Higher Education Priority Development Areas (20111402130002).

Reference

[1] J.J. Spivey and A. Egbebi, Chem. Soc. Rev. 2007, 36, 1514-1528.

199 [2] V. Subramani and S.K. Gangwal, Energy Fuels, 2008, 22, 814-839.

200 [3] J.J. Wang, P.A. Chernavskii, A.Y. Khodakov and Y. Wang, J. Catal., 2012, 286, 51-61.

201 [4] K. Xiao, Z.H. Bao, X.Z. Qi, X.X. Wang, L.S. Zhong, M.G. Lin, K.G. Fang and Y.H. Sun, Catal.

202 Commun., 2013, 40, 154-157.

203 [5] E. Heracleous, E.T. Liakakou, A.A. Lappas and A.A. Lemonidou, Appl. Catal. A: Gen. 2013,

204 455, 145-154.

205 [6] M. Gupta, M.L. Smith and J.J. Spivey, ACS Catal., 2011, 1, 641-656.

206 [7] K.G. Fang, D.B. Li, M.G. Lin, M.L. Xiang, W. Wei and Y.H. Sun, Catal. Today, 2009, 147,

207 133-138.

208 [8] M. Behrens, F. Studt, I. Kasatkin, S. Kühl, M. Hävecker, F. Abild-Pedersen, S. Zander, F.

209 Girgsdies, P. Kurr, B.L. Kniep, M. Tovar, R.W. Fischer, J.K. Nørskov and R. Schlögl, Science,

210 2012, 336, 893-897.

211 [9] Y. Yang, J. Evans, J.A. Rodriguez, M.G. White, P. Liu, Phys. Chem. Chem. Phys. 2010, 12,

212 9909-9917.

213 [10] W. Huang, L.M. Yu, W.H. Li and Z.L. Ma, Front. Chem. Eng. China, 2010, 4, 472- 475.

214 [11] Z.J. Zuo, L. Wang, Y.J. Liu and W. Huang, Catal. Commun., 2013, 34, 69-72.

215 [12] Z. J. Zuo, L. Wang, L.M. Yu, P.D. Han and W. Huang, J. Phys. Chem. C., 2014, 118,

216 12890-12898.

217 [13] Z. Tang, J.L. Liang, X.H. Li, J.F. Li, H.L. Guo, Y.Q. Liu and C.G. Liu, J. Solid State Chem.,

218 2013, 202, 305-314.

219 [14] L.M Zhang, W.C. Lu, R.R. Cui and S.S. Shen, Mater. Res. Bull., 2010, 45, 429-436.

220 [15] Z.J. Wang, H. Du, J.H. Gong, S.G. Yang, J.H. Ma and J. Xu. Colloid. Surf. A-Physicochem.

Eng. Asp., 2014, 450, 76-82.

[16] G. Busca, Catal. Today, 2014, 226, 2-13.

[17] F.J. Berry, R.L. Bilsborrow, A.J. Dent, M. Mortimer, C.B. Ponton, B.J. Purser and K.R. Whittle, Polyhedron, 1999, 18, 1083-1087.

[18] S. Jiansirisomboon and K.J.D. MacKenzie, Mater. Res. Bull., 2006, 41, 791-803.

[19] Z.H. Gao, W. Huang, L.H. Yin and K.C. Xie, Fuel Process. Technol., 2009, 90, 1442-1446.

[20] P. Gao, F. Li, H.J Zhan, N. Zhao, F.K. Xiao, W. Wei, L.S. Zhong, H. Wang and Y.H. Sun, J. Catal., 2013, 298, 51-60.

[21] T. Isobe, M. Shimizu, S. Matsushita and A. Nakajima, J. Asian Ceram. Soc., 2013, 1, 65-70.

[22] Y.F. Zhou, H.Y. Fu, X.J. Zheng, R.X. Li, H. Chen and X.J. Li, Catal. Commun., 2009, 11, 137-141.

[23] C. Baltes, S. Vukojevic and F. Schüth, J. Catal., 2008, 258, 334-344.

[24] K. Xiao, Z.H. Bao, X.Z. Qi, X.X Wang, L.S. Zhong, K.G. Fang, M.G. Lin and Y.H. Sun, J. Mol. Catal. A, 2013, 378, 319-325.

[25] S.Z. Li, W.P. Ding, G.D. Meitzner and E. Iglesia, J. Phys. Chem. B, 2002, 106, 85-91.

Table Captions

Table 1 Catalytic performance of Cu-Zn-Al catalyst.

Table 2 Product distributions of Cu-Zn-Al catalyst.

Table 3 The composition of Cu-Zn-Al catalyst before and after reaction.

Table 4 XPS parameters of the Cu-Zn-Al catalyst before and after reaction.

Table 5 Catalytic performance of Cu-ZnO-Al_2O_3 catalyst.

Table 6 Product distributions of Cu-ZnO-Al_2O_3 catalyst.

Figure captions

Fig. 1. XRD patterns of Cu-Zn-Al catalyst. (a) before reaction (b) after reaction

Fig. 2. FTIR spectra of Cu-Zn-Al catalyst. (a) before reaction (b) after reaction

Fig. 3. NH_3-TPD-MS profile of Cu-Zn-Al catalyst. (a) before reaction (b) after reaction

Fig. 4. ^{27}Al-MAS-NMR spectra of Cu-Zn-Al catalyst. (a) before reaction (b) after reaction

Fig. 5. Cu 2p XPS spectra of Cu/Zn/Al catalyst. (a) before reaction (b) after reaction

Fig.6. TG-DTG profiles of Cu/Zn/Al catalyst. (a) before reaction (b) after reaction

287 **Table 1** Catalytic performance of Cu-Zn-Al catalyst

Time/h	CO Conversion (%)	Selectivity (wt. %)				C_{2+}OH/ROH (%)
		ROH	HC	DME	CO_2	
24	19.8	31.4	18.4	1.37	48.8	36.0
48	38.9	15.4	28.7	4.53	51.3	68.6
72	35.2	14.0	32.9	12.6	40.6	56.7
96	33.8	19.1	25.2	17.6	38.1	28.6
120	32.0	22.1	25.7	17.9	34.2	14.1

288 Notes: Reaction conditions: T=523 K, P=4.5 MPa, H_2/CO=2, feed low rate= 150 mL/min, ROH
289 for total alcohols and HC for hydrocarbon, C_{2+}OH/ROH for higher alcohols selectivity.

290
291
292
293
294
295
296
297
298
299
300
301

Table 2 Product distributions of Cu-Zn-Al catalyst

Time/h	ROH distribution (wt. %)					HC distribution (wt. %)				
	MEOH	ETOH	PrOH	BuOH	PeOH	C1	C2	C3	C4	$C5^+$
24	64.0	20.3	5.8	7.3	2.6	29.7	33.8	17.5	15.2	3.8
48	31.4	38.7	13.3	12.8	3.8	36.0	28.6	16.2	13.5	5.7
72	43.3	25.8	10.9	13.7	6.3	43.0	22.3	15.3	12.2	7.1
96	71.4	11.5	4.6	9.0	3.5	45.4	23.4	14.9	11.1	5.2
120	85.9	3.6	2.0	7.0	1.5	44.3	24.2	14.6	11.3	5.7

317 **Table 3** The composition of Cu-Zn-Al catalyst before and after reaction

Catalyst	GF AAS (mg/L)		
	Cu	Zn	Al
before reaction	0.430	0.238	0.029
after reaction	0.408	0.240	0.032

318

319

320

321

322

323

324

325

326

327

328

329

330

331

332

333

334

335 **Table 4** XPS parameters of the Cu-Zn-Al catalyst before and after reaction

Metal component	Binding energy (eV)	
	before reaction	after reaction
Cu2$p_{3/2}$	932.0	932.1
Zn2$p_{3/2}$	1021.7	1020.6
Al2p	74.5	73.7

336

337

338

339

340

341

342

343

344

345

346

347

348

349

350

351

352 **Table 5** Catalytic performance of Cu-ZnO-Al_2O_3 catalyst

Catalyst	CO Conversion (%)	Selectivity (wt. %)				C_{2+}OH/ROH (%)
		ROH	HC	DME	CO2	
Cu-ZnO-Al_2O_3	24.7	48.1	5.5	24.6	21.8	7.2

353 Notes: Reaction conditions: T=523 K, P=4.5 MPa, H_2/CO=2, feed low rate= 150 mL/min, ROH

354 for total alcohols and HC for hydrocarbon, C_{2+}OH/ROH for higher alcohols selectivity.

355

356

357

358

359

360

361

362

363

364

365

366

367

368

369

370

371 **Table 6** Product distributions of Cu-ZnO-Al_2O_3 catalyst

Catalyst	ROH distribution (wt. %)					HC distribution (wt. %)				
	MEOH	ETOH	PrOH	BuOH	PeOH	C1	C2	C3	C4	C5+
Cu-ZnO-Al_2O_3	92.8	2.9	1.0	2.2	1.1	31.7	22.4	20.8	16.8	8.2

372

373

374

375

376

377

378

379

380

381

382

383

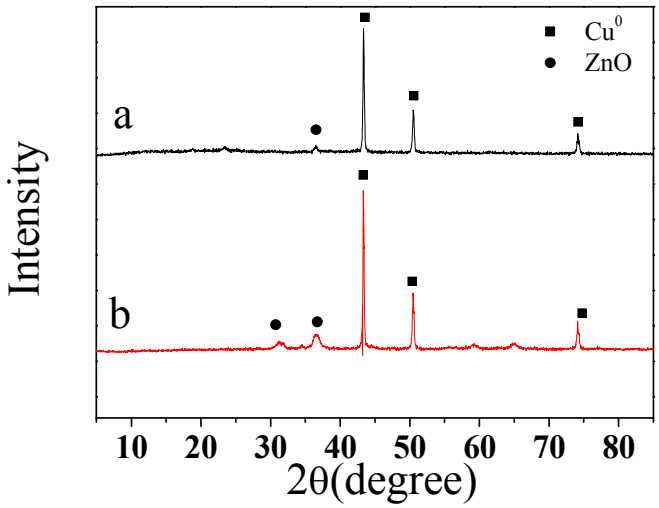

Fig. 1. XRD patterns of Cu-Zn-Al catalyst. (a) before reaction (b) after reaction

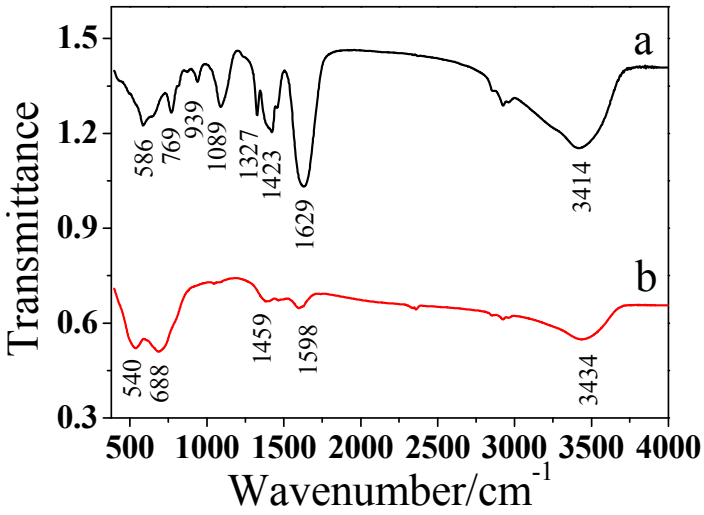

Fig. 2. FTIR spectra of Cu-Zn-Al catalyst. (a) before reaction (b) after reaction

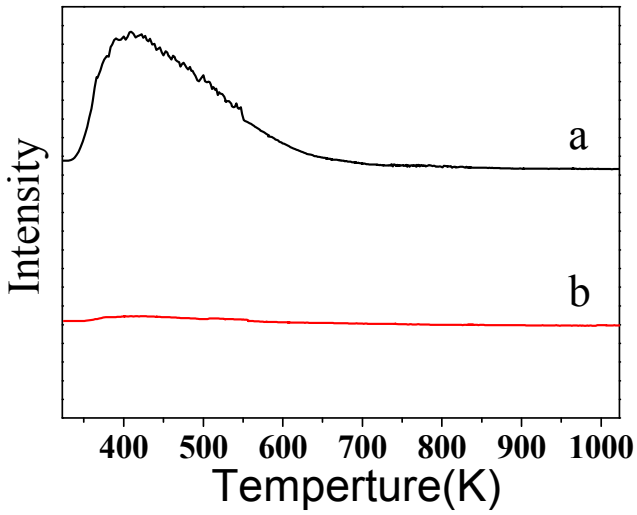

414

415 **Fig. 3.** NH_3-TPD-MS profile of Cu-Zn-Al catalyst. (a) before reaction (b) after reaction

416

417

418

419

420

421

422

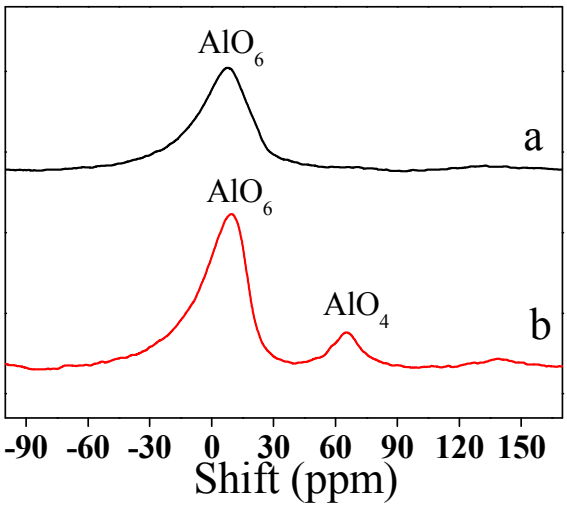

Fig. 4. ^{27}Al-MAS-NMR spectra of Cu-Zn-Al catalyst. (a) before reaction (b) after reaction

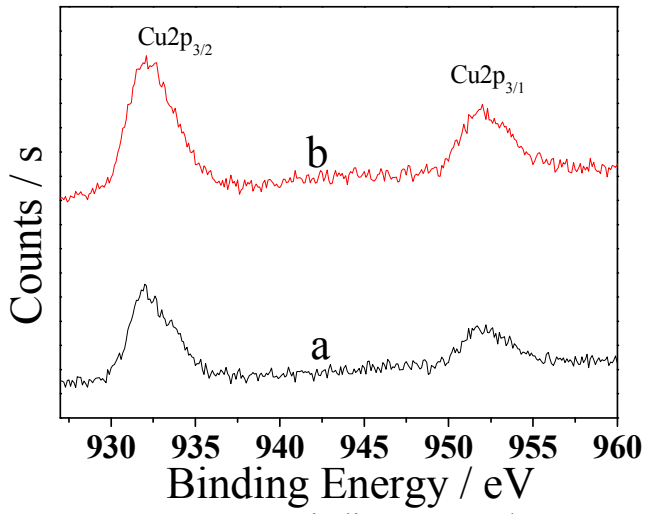

439

440 **Fig. 5.** Cu 2p XPS spectra of Cu/Zn/Al catalyst. (a) before reaction (b) after reaction

441

442

443

444

445

446

447

448

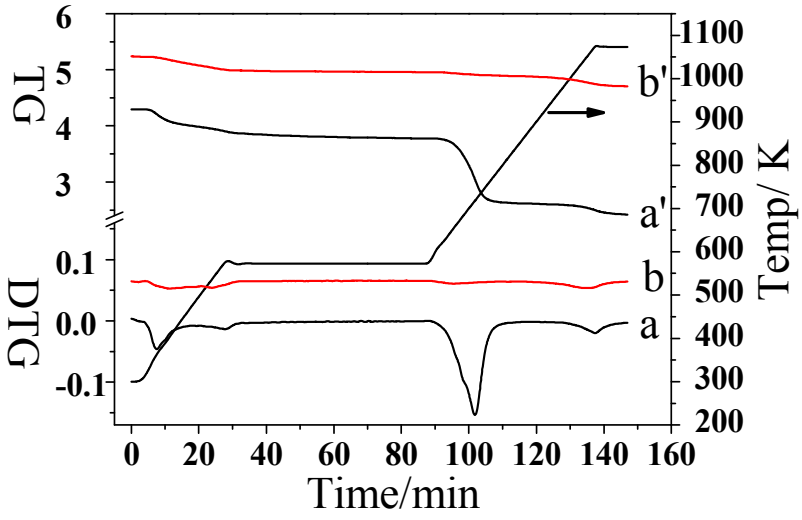

449

450 **Fig.6.** TG-DTG profiles of Cu/Zn/Al catalyst. (a) before reaction (b) after reaction

Graphical abstract